JACS
JOURNAL OF THE AMERICAN CHEMICAL SOCIETY
Communication
pubs.acs.org/JACS

Influence of Electronic Spin and Spin–Orbit Coupling on Decoherence in Mononuclear Transition Metal Complexes

Michael J. Graham,[†] Joseph M. Zadrozny,[†] Muhandis Shiddiq,[‡] John S. Anderson,[†] Majed S. Fataftah,[†] Stephen Hill,*[,‡] and Danna E. Freedman*[,†]

[†]Department of Chemistry, Northwestern University, Evanston, Illinois 60208-3113, United States
[‡]National High Magnetic Field Laboratory, Tallahassee, Florida 32310, United States

Supporting Information

ABSTRACT: Enabling the rational synthesis of molecular candidates for quantum information processing requires design principles that minimize electron spin decoherence. Here we report a systematic investigation of decoherence via the synthesis of two series of paramagnetic coordination complexes. These complexes, $[M(C_2O_4)_3]^{3-}$ (M = Ru, Cr, Fe) and $[M(CN)_6]^{3-}$ (M = Fe, Ru, Os), were prepared and interrogated by pulsed electron paramagnetic resonance (EPR) spectroscopy to assess quantitatively the influence of the magnitude of spin ($S = {}^1/_2, {}^3/_2, {}^5/_2$) and spin–orbit coupling (ζ = 464, 880, 3100 cm^{-1}) on quantum decoherence. Coherence times (T_2) were collected via Hahn echo experiments and revealed a small dependence on the two variables studied, demonstrating that the magnitudes of spin and spin–orbit coupling are not the primary drivers of electron spin decoherence. On the basis of these conclusions, a proof-of-concept molecule, $[Ru(C_2O_4)_3]^{3-}$, was selected for further study. The two parameters establishing the viability of a qubit are a long coherence time, T_2, and the presence of Rabi oscillations. The complex $[Ru(C_2O_4)_3]^{3-}$ exhibits both a coherence time of T_2 = 3.4 μs and the rarely observed Rabi oscillations. These two features establish $[Ru(C_2O_4)_3]^{3-}$ as a molecular qubit candidate and mark the viability of coordination complexes as qubit platforms. Our results illustrate that the design of qubit candidates can be achieved with a wide range of paramagnetic ions and spin states while preserving a long-lived coherence.

The realization of quantum information processing (QIP) is a fundamental challenge with important contributions arising from the intersection of chemistry and physics. Indeed, particular attention is warranted from chemists because a quantum computer could accurately simulate the quantum behavior of chemical systems.[1] While many systems have been proposed for QIP,[2] electronic spin represents a promising approach to quantum bits, or qubits.[3] Electronic spin-based QIP employs transitions between M_S levels that can be simply addressed by electron paramagnetic resonance (EPR) spectroscopy. Utilizing electronic spin as a qubit offers a key advantage, namely, that a single parameter, zero-field splitting, creates a manifold of separately addressable transitions, each one a qubit. The inherent scalability and tunability engendered by zero-field splitting are illustrated in Figure 1, which depicts a molecule with spin quantum number S possessing $2S+1$ M_S states and $S(2S+1)$ unique transitions between pairs of those states that could be utilized as qubits.[4] As zero-field splitting is a synthetically tunable property of high-spin transition metal complexes that splits M_S levels by energies determined by axial (D) and transverse (E) components, it ensures uniqueness of the energies of each of the $S(2S+1)$ qubits.[3,5,6] Scalability in electron-based QIP is further enabled by the relative strength of magnetic superexchange coupling relative to nuclear-spin systems, thus creating potentially strong interqubit interactions over long distances.[7] The simultaneous realization of scalability and tunability in electron spin qubits demonstrates their promise for the implementation of quantum computation.[8,9]

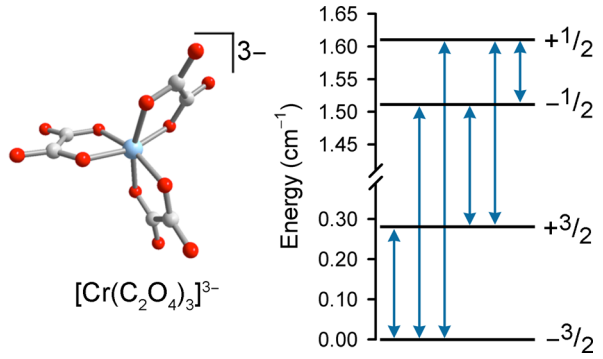

Figure 1. (Left) Molecular structure of $[Cr(C_2O_4)_3]^{3-}$. Light blue, red, and gray spheres represent chromium, oxygen, and carbon atoms, respectively. (Right) Splitting of the M_S levels of the $S = {}^3/_2$ moment in $[Cr(C_2O_4)_3]^{3-}$, calculated for g_z = 1.99, D = −0.71 cm^{-1}, E = 0 cm^{-1} (see Supporting Information) under a static 1000 Oe dc field parallel to the z-axis. Blue arrows indicate the six potential qubits in $[Cr(C_2O_4)_3]^{3-}$.[4]

The primary challenge in realizing electronic spin-based QIP lies in developing a long coherence lifetime for the qubit, T_2,[10] relative to the time scale of a computational cycle.[9,11] This is a particular challenge for electronic spin-based QIP because T_2 values for electron spins are typically short.[7,8,12,13] Yet, theoretical estimates of achievable coherence times[14] suggest that long coherence times are within a synthetically tunable range. Thus, the preparation of molecules with long coherence times is a valuable design target for inorganic chemists.

Received: April 14, 2014
Published: May 16, 2014

   dx.doi.org/10.1021/ja5037397 | J. Am. Chem. Soc. 2014, 136, 7623–7626

Rational synthesis of molecular qubits necessitates the ability to design molecules with long coherence times. Connecting electronic and molecular structure with decoherence would give rise to design principles that could be followed for the preparation of long-lived electron spin qubits. Two aspects of the electronic structure of paramagnetic complexes that are essential for tuning the qubit transition manifold are S and spin−orbit coupling (SOC).[15] Notably, both of these have also been implicated as major facilitators of decoherence.[7,16−19] Indeed, the presence of a larger S increases the contribution of electronic dipolar decoherence mechanisms to the overall decoherence rate,[7,16] while greater SOC allows more rapid decoherence by enhancing coupling between lattice phonons and spin.[20] To the best of our knowledge, however, rigorous experimental examination of the contribution of these processes to decoherence under conditions relevant to QIP is lacking. Herein, we report a systematic investigation of the influence of spin magnitude and SOC on coherence times in six paramagnetic transition metal complexes and demonstrate proof-of-concept with a new candidate qubit.

Six molecules were selected for a systematic study of decoherence comprising two series, one varying the magnitude of S and the other varying SOC (see Figure 2). The complexes

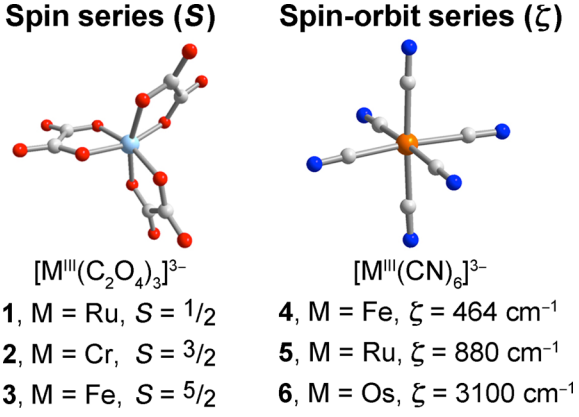

Figure 2. Depictions of the molecular structures of the spin series **1**−**3** (left) and spin−orbit series **4**−**6** (right). Red, blue, and gray spheres represent oxygen, nitrogen, and carbon atoms, respectively. The central light blue and orange spheres represent the varying metal atoms.

selected were $K_3[Ru(C_2O_4)_3]$ (**1**),[21] $K_3[Cr(C_2O_4)_3]$ (**2**),[22] $K_3[Fe(C_2O_4)_3]$ (**3**), $(Ph_4P)_3[Fe(CN)_6]$ (**4**),[23] $(Ph_4P)_3[Ru(CN)_6]$ (**5**),[24] and $(Ph_4P)_3[Os(CN)_6]$ (**6**).[25] Molecules **1**−**3** and **4**−**6** vary spin magnitude and SOC, respectively. The complexes of **1**−**3** possess spin states of $S = {}^1/_2$, ${}^3/_2$, and ${}^5/_2$, whereas those of **4**−**6** are all $S = {}^1/_2$ but feature increasing free-ion SOC constants of 464, 880, and 3100 cm^{-1} (see Figure S1 in Supporting Information).[23b,24a,25]

These compounds were meticulously selected to create systematic variation of the desired property while maintaining other features of the electronic structure. Importantly, octahedral coordination environments were maintained throughout both series, although the oxalate complexes do deviate from perfect octahedral symmetry. Within each series uniform ligand fields were employed to reduce variation in the structural and electronic properties. All of these molecules possess half-integer spin states, allowing more facile EPR spectroscopic characterization. To eliminate complications arising from nuclear spin-based decoherence within the molecules, complexes in a zero nuclear spin ligand field were selected for the spin series of compounds, while the SOC series employed ligands with nitrogen as the only spin-active nucleus.[8,20,26,27] All metals selected contain a low natural abundance of spin-active isotopes. However, nuclear spin could not be removed from the solvents, and that will be the subject of a future study. Within the spin series **1**−**3**, it was not possible to completely control for the variation of SOC, as it varies with element and oxidation state.[5] However, the larger spin−orbit coupling of compound **1** compared with compounds **2** and **3** provided a useful intersection point between the two series and allowed for a direct comparison of the effects of both properties of interest. Compounds **1**−**6** were prepared following literature methods, with the exception of **3**, which was used as received. However, the synthesis of **5** required substantial modification of the original procedure (see p S4 of Supporting Information).[24a]

Coherence times (T_2) for frozen 1 mM solutions of **1**−**6** in 1:1 (v/v) H_2O/glycerol were extracted from data obtained by application of a two-pulse Hahn echo sequence at temperatures ranging from 5 to 22 K. The pulse sequence we employed is depicted in Figure 3. Cw-EPR spectra were acquired to

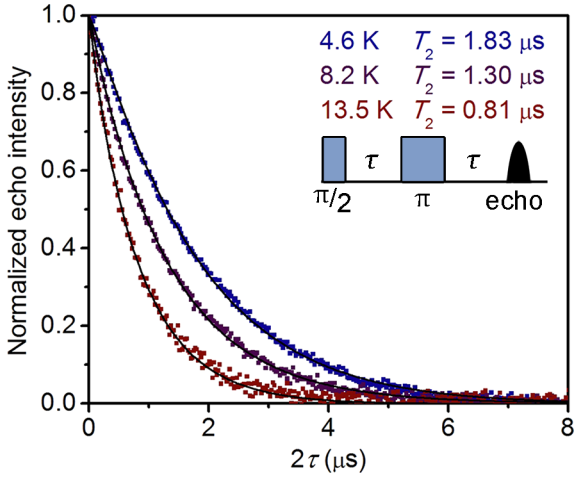

Figure 3. Normalized decay curves for **3** in 1:1 H_2O/glycerol and graphical depiction of the Hahn echo pulse sequence. The black lines represent stretched exponential functions fit to the data.

determine zero-field splitting parameters for **2** and **3** (see Figures S10−S13 in Supporting Information). Echo intensities were recorded as a function of dc applied field (see Figure S2 in Supporting Information). In each echo-detected field-swept spectrum, a maximum in the echo intensity was observed at the dc fields listed in Table 1. Echo decay curves were subsequently acquired on all samples at the field of maximum echo intensity (see Figures S3−S8 in Supporting Information). Echo intensities decayed with increasing interpulse delay times (τ) for all complexes, and the rate of decay increased with increasing temperature (see Figure 3). Quantitation of T_2 proceeded by fitting the decay of the echo intensity by a stretched exponential function, $I(2\tau) = I(0)\exp(-(2\tau/T_2)^x)$, where I is the echo intensity, $I(0)$ a pre-exponential factor, and x the stretch factor, while τ and T_2 possess their previously defined meanings. Values of T_2 obtained from the best fits to the data are listed in Table 1. For **1**−**3**, T_2 decreases slightly at 5 K from 3.44(1) in **1** to 1.83(1) μs in **3**. T_2 values slightly increase from **4** to **6**, ranging from 2.38(6) to 4.12(6) μs at 5 K.

dx.doi.org/10.1021/ja5037397 | J. Am. Chem. Soc. 2014, 136, 7623−7626

Table 1. Magnetic Parameters and T_2 values[a] for 1−6

	1	2	3
S	$^1/_2$	$^3/_2$	$^5/_2$
H_{dc} (Oe)[b]	2812	2130	3501
T_2 at 5 K	3.44(1)	2.79(3)	1.83(1)
T_2 at 14 K	2.01(1)	1.86(3)	0.81(1)
T_2 at 22 K	0.41(2)	1.27(4)	0.45(5)
	4	**5**	**6**
S	$^1/_2$	$^1/_2$	$^1/_2$
ζ (cm^{-1})[c]	464	880	3100
H_{dc} (Oe)[b]	3364	3394	3865
T_2 at 5 K	2.38(6)	2.55(4)	4.12(6)
T_2 at 13 K	0.55(8)	1.25(5)	3.17(4)
T_2 at 22 K	0.60(9)	1.29(10)	1.04(4)

[a]In units of μs, as determined on 1 mM solutions in 1:1 H_2O/glycerol. [b]Dc applied field at highest echo intensity. [c]Free-ion values from refs 23b, 24a, and 25.

These values of T_2 for **1**−**6** are comparable in magnitude to those of other mononuclear transition metal complexes.[28]

Insight into the impact of spin magnitude on decoherence can be attained through comparison of the T_2 values across **1**−**3**. The results confirm that increasing spin magnitude impacts decoherence: **1** displayed the longest T_2 values, followed by **2** and then **3**. Thus, the trend in our data is in accordance with expected results: a larger spin magnitude will increase the strength of intermolecular dipolar interactions and enhance the contribution of both electronic and nuclear dipolar flip-flops to the decoherence rate.[7,16,19,29] However, notably, although T_2 decreases with increasing spin, the difference between **3** and **1** at 5 K is only a factor of ∼2. The small magnitude of the decrease allows the molecules possessing the largest spins to display coherence times within the microsecond regime, a relatively long-lived state. These results demonstrate that in the concentration regime appropriate for signal detection, spin magnitude can be varied without significantly compromising T_2.

Comparison of the T_2 values for **4**−**6** elucidates the influence of SOC, the magnitude of which increases dramatically in the order Fe^{III} < Ru^{III} < Os^{III}. The magnitude of T_2 was expected to decrease in that order, owing to the fact that SOC mediates spin−lattice relaxation, a contributor to decoherence. However, the shortest T_2 value observed at 5 K is for **4**, followed by **5**, and then **6** (see Table 1). This trend is the opposite of the expected dependence, and thus the operative mechanisms for decoherence in **4**−**6** are not strongly dependent on variations in SOC. The T_2 of **1** supports this notion, as **1** exhibits the longest coherence time of the spin series despite having the greatest degree of SOC in that set. These results highlight the fact that one need not focus on low-ζ ions when synthesizing new electron spin qubits. On the basis of these results, we hypothesize that the primary driver of decoherence in these systems is the frequently implicated nuclear spin-based decoherence.[7,8,11]

In order to validate the design principles set out above, we selected a species, $[Ru(C_2O_4)_3]^{3-}$, with substantial spin−orbit coupling, for evaluation as a qubit. The two conditions required for a successful electron spin qubit are the presence of a sufficiently long T_2 and the ability to place the potential qubit into any arbitrary superposition of its two constituent states. This property, known as coherent spin dynamics, is unusual and has been observed in only a small number of molecular species.[13,18,19,30] Its existence is demonstrated by transient nutation experiments, in which an applied pulse of varying length, t_p, places the qubit into a specific superposition state determined by the pulse length. After a fixed delay much greater than T_2, a two-pulse Hahn echo sequence is used to detect the echo intensity (see Figure 4).[29,30]

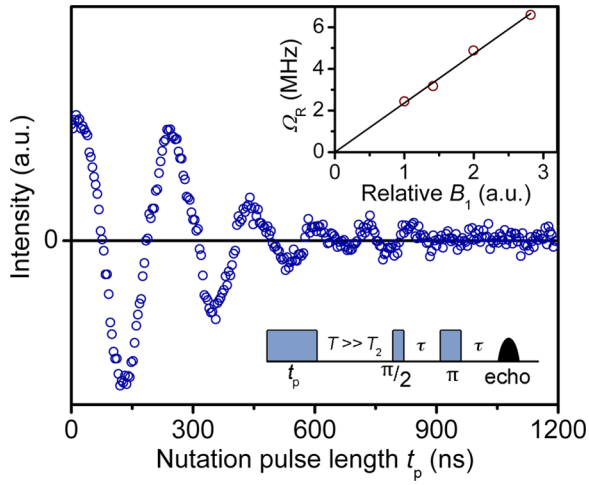

Figure 4. Rabi oscillations and pulse sequence for a solution of **1** at 5 K, H_{dc} = 2812 G, and relative B_1 of 2.0. Inset: Rabi frequency of oscillations from **1** as a function of the pulsed field strength relative to the lowest employed B_1.

If the molecule is viable as a qubit, the echo intensity will display a continuous, decaying oscillation (known as a Rabi oscillation) as the system cycles through superposition states.[13,30b] As electron spin echo envelope modulation (ESEEM)[29] or cavity effects[30a] can also impart oscillating t_p dependence to the echo intensity, it is necessary to record nutation data at multiple pulse powers. The frequency of a Rabi oscillation, the Rabi frequency (Ω_R), will increase linearly with the pulsed field strength B_1, in contrast to ESEEM, for which the frequency remains constant.[29] As shown in Figure 4, Fourier transforms of the oscillations of **1** recorded at multiple powers reveal a linear relationship between B_1 and Ω_R. Thus, the $M_S = -^1/_2 \leftrightarrow M_S = +^1/_2$ transition in complex **1** can be successfully placed into any arbitrary superposition, and the transition does, in fact, behave as an electron spin qubit. To our knowledge, this marks the first observation of Rabi oscillations in a second- or third-row transition metal complex.

The foregoing study demonstrated via measurement of **1**−**6** that variation in spin and SOC is viable without significant impact on coherence time. One key advantage of electronic spin-based qubits is the ability to synthesize a single molecule containing multiple qubits by tuning zero-field splitting and spin. Since rational synthesis of molecules with a manifold of separately addressable transitions relies upon careful synthetic tuning of spin and SOC, our results illustrate the viability of mononuclear transition metal molecules as QIP candidates. Observation of Rabi oscillations in a second-row transition metal complex further bolsters this conclusion. Taken together, these results provide a first step toward a set of guidelines for the future development of an electron spin-based molecular qubit. Future research will focus on the synthesis and measurement of nuclear spin-free mononuclear transition metal complexes and the quantification of nuclear spin-based decoherence.

dx.doi.org/10.1021/ja5037397 | J. Am. Chem. Soc. 2014, 136, 7623−7626

■ ASSOCIATED CONTENT

Supporting Information

Full experimental details, additional magnetic and spectroscopic characterization data, and CIFs for **4** and **5**. This material is available free of charge via the Internet at http://pubs.acs.org.

■ AUTHOR INFORMATION

Corresponding Authors

shill@magnet.fsu.edu
danna.freedman@northwestern.edu

Notes

The authors declare no competing financial interest.

■ ACKNOWLEDGMENTS

We thank Prof. T. D. Harris, Dr. L. Song, and S. Ling for experimental assistance. We acknowledge support from Northwestern University and the Institute for Sustainability and Energy at Northwestern University (ISEN) (Booster Award 10031846). The NSF (DMR-1309463) and the United States Air Force (AOARD award no. 134031) funded data acquisition and analysis at the National High Magnetic Field Laboratory (NHMFL). A seed grant from the MRSEC program of the NSF at Northwestern University (DMR-1121262) enabled the study of magnetic anisotropy in these systems. Magnetic measurements were partially enabled by funding from the International Institute for Nanotechnology and the State of Illinois DCEO Award no. 10-203031. The NHMFL is supported by NSF Cooperative Agreement (DMR-0654118) and by Florida.

■ REFERENCES

(1) (a) Aspuru-Guzik, A.; Dutoi, A. D.; Love, P. J.; Head-Gordon, M. *Science* **2005**, *309*, 1704−1707. (b) Feynman, R. P. *Int. J. Theor. Phys.* **1982**, *21*, 467−488.

(2) (a) Stolze, J.; Suter, D. *Quantum Computing: A Short Course from Theory to Experiment*, 2nd ed.; Wiley-VCH Verlag GmbH & Co. KGaA: Weinheim, 2008. (b) Vandersypen, L. M. K.; Steffen, M.; Breyta, G.; Yannoni, C. S.; Sherwood, M. H.; Chuang, I. L. *Nature* **2001**, *414*, 883−887.

(3) Leuenberger, M. N.; Loss, D. *Nature* **2001**, *410*, 789−793.

(4) Though three of the six transitions depicted in Figure 1 are formally forbidden, the frequent observation of forbidden transitions in EPR spectra allows for their consideration as potential qubits.

(5) Figgis, B. N.; Hitchman, M. A. *Ligand Field Theory and Its Applications*; Wiley-VCH: New York, 2000.

(6) Kahn, O. *Molecular Magnetism*; VCH Publishers: New York, 1993.

(7) Stamp, P. C. E.; Gaita-Ariño, A. *J. Mater. Chem.* **2009**, *19*, 1718−1730.

(8) Wedge, C. J.; Timco, G. A.; Spielberg, E. T.; George, R. E.; Tuna, F.; Rigby, S.; McInnes, E. J. L.; Winpenny, R. E. P.; Blundell, S. J.; Ardavan, A. *Phys. Rev. Lett.* **2012**, *108*, 107204.

(9) Aromí, G.; Aguilà, D.; Gamez, P.; Luis, F.; Roubeau, O. *Chem. Soc. Rev.* **2012**, *41*, 537−546.

(10) The phase memory time is also often represented as T_m; see refs 20 and 29.

(11) Ardavan, A.; Rival, O.; Morton, J. J. L.; Blundell, S. J.; Tyryshkin, A. M.; Timco, G. A.; Winpenny, R. E. P. *Phys. Rev. Lett.* **2007**, *98*, 057201.

(12) Wang, Z.; Datta, S.; Papatriantafyllopoulou, C.; Christou, G.; Dalal, N. S.; van Tol, J.; Hill, S. *Polyhedron* **2011**, *30*, 3193−3196.

(13) Schlegel, C.; van Slageren, J.; Manoli, M.; Brechin, E. K.; Dressel, M. *Phys. Rev. Lett.* **2008**, *101*, 147203.

(14) Takahashi, S.; Tupitsyn, I. S.; van Tol, J.; Beedle, C. C.; Hendrickson, D. N.; Stamp, P. C. E. *Nature* **2011**, *476*, 76−79.

(15) (a) Gatteschi, D.; Sessoli, R.; Villain, J. *Molecular Nanomagnets*; Oxford University Press: New York, 2006. (b) Pedersen, K. S.; Bendix, J.; Clérac, R. *Chem. Commun.* **2014**, *50*, 4396−4415. (c) Christou, G.; Gatteschi, D.; Hendrickson, D. N.; Sessoli, R. *MRS Bull.* **2000**, *25*, 66−71. (d) Shatruk, M.; Avendano, C.; Dunbar, K. R. *Prog. Inorg. Chem.* **2009**, 155−334.

(16) (a) Morello, A.; Stamp, P. C. E.; Tupitsyn, I. S. *Phys. Rev. Lett.* **2006**, *97*, 207206. (b) Stamp, P. C. E.; Tupitsyn, I. S. *Phys. Rev. B* **2004**, *69*, 014401.

(17) (a) Wolf, S. A.; Awschalom, D. D.; Buhrman, R. A.; Daughton, J. M.; von Molnár, S.; Roukes, M. L.; Chtchelkanova, A. Y.; Treger, D. M. *Science* **2001**, *294*, 1488−1495. (b) Zheng, Y.; Wudl, F. *J. Mater. Chem. A* **2014**, *2*, 48−57. (c) Lee, E. C.; Choi, Y. C.; Kim, W. Y.; Singh, N. J.; Lee, S.; Shim, J. H.; Kim, K. S. *Chem.—Eur. J.* **2010**, *16*, 12141−12146. (d) Nuccio, L.; Willis, M.; Schulz, L.; Fratini, S.; Messina, F.; D'Amico, M.; Pratt, F. L.; Lord, J. S.; McKenzie, I.; Loth, M.; Purushothaman, B.; Anthony, J.; Heeney, M.; Wilson, R. M.; Hernández, I.; Cannas, M.; Sedlak, K.; Kreouzis, T.; Gillin, W. P.; Bernhard, C.; Drew, A. J. *Phys. Rev. Lett.* **2013**, *110*, 216602.

(18) Warner, M.; Din, S.; Tupitsyn, I. S.; Morley, G. W.; Stoneham, A. M.; Gardener, J. A.; Wu, Z.; Fisher, A. J.; Heutz, S.; Kay, C. W. M.; Aeppli, G. *Nature* **2013**, *503*, 504−508.

(19) Bertaina, S.; Gambarelli, S.; Mitra, T.; Tsukerblat, B.; Müller, A.; Barbara, B. *Nature* **2008**, *453*, 203−206.

(20) Eaton, S. S.; Eaton, G. R. In *Biological Magnetic Resonance*; Berliner, L. J., Eaton, S. S., Eaton, G. R., Eds.; Klewer Academic/Plenum Publishers: New York, 2000; Vol. *19*, Distance Measurements in Biological Systems by EPR, pp 29−154.

(21) (a) Kaziro, R.; Hambley, T. W.; Binstead, R. A.; Beattie, J. K. *Inorg. Chim. Acta* **1989**, *164*, 85−91. (b) Larionova, J.; Mombelli, B.; Sanchiz, J.; Kahn, O. *Inorg. Chem.* **1998**, *37*, 679−684.

(22) Bailar, J. C., Jr.; Jones, E. M.; Booth, H. S.; Grennert, M. *Inorg. Synth.* **1939**, *1*, 35−38.

(23) (a) Schmidtke, H.-H.; Eyring, G. *Z. Phys. Chem.* **1974**, *92*, 211−222. (b) Bendix, J.; Brorson, M.; Schäffer, C. E. *Inorg. Chem.* **1993**, *32*, 2838−2849.

(24) (a) Bendix, J.; Steenberg, P.; Søtofte, I. *Inorg. Chem.* **2003**, *42*, 4510−4512. (b) Vostrikova, K. E.; Peresypkina, E. V. *Eur. J. Inorg. Chem.* **2011**, 811−815.

(25) Albores, P.; Slep, L. D.; Baraldo, L. M.; Baggio, R.; Garland, M. T.; Rentschler, E. *Inorg. Chem.* **2006**, *45*, 2361−2363.

(26) Ochsenbein, S. T.; Gamelin, D. R. *Nat. Nanotechnol.* **2011**, *6*, 112−115.

(27) Although measurement of T_2 in a protiated solvent matrix likely nullifies much of the effect of removing nuclear spins from the system, this consideration was still taken due to the ease of changing solvent systems and the comparative difficulty of ligand substitution.

(28) (a) Eaton, G. R.; Eaton, S. S. *J. Magn. Reson.* **1999**, *136*, 63−68. (b) Fielding, A. J.; Fox, S.; Millhauser, G. L.; Chattopadhyay, M.; Kroneck, P. M. H.; Fritz, G.; Eaton, G. R.; Eaton, S. S. *J. Magn. Reson.* **2006**, *179*, 92−104. (c) Krupskaya, Y.; Zaripov, R.; Vavilova, E.; Miluykov, V.; Bezkishko, I.; Krivolapov, D.; Kataeva, O.; Sinyashin, O.; Hey-Hawkins, E.; Voronkova, V.; Salikhov, K.; Kataev, V.; Büchner, B. *Phys. Rev. B* **2011**, *84*, 092402.

(29) Schweiger, A.; Jeschke, G. *Principles of Pulse Electron Paramagnetic Resonance*; Oxford University Press: New York, 2001.

(30) (a) Yang, J.; Wang, Y.; Wang, Z.; Rong, X.; Duan, C.-K.; Su, J.-H.; Du, J. *Phys. Rev. Lett.* **2012**, *108*, 230501. (b) Moro, F.; Kaminski, D.; Tuna, F.; Whitehead, G. F. S.; Timco, G. A.; Collison, D.; Winpenny, R. E. P.; Ardavan, A.; McInnes, E. J. L. *Chem. Commun.* **2014**, *50*, 91−93. (c) Baldoví, J. J.; Cardona-Serra, S.; Clemente-Juan, J. M.; Coronado, E.; Gaita-Ariño, A.; Prima-García, H. *Chem. Commun.* **2013**, *49*, 8922−8924. (d) Mitrikas, G.; Sanakis, Y.; Raptopoulou, C. P.; Kordas, G.; Papavassiliou, G. *Phys. Chem. Chem. Phys.* **2008**, *10*, 743−748.